J Electroceram (2010) 24:288–293
DOI 10.1007/s10832-009-9570-2

Design of thin cross type ultrasonic motor

Taegone Park · Seongsu Jeong · Hyonho Chong · Kenji Uchino

Received: 3 February 2008 / Accepted: 24 March 2009 / Published online: 9 April 2009

Abstract This paper proposes a newly designed structure for a thin ultrasonic rotary motor. A thin brass plate is used as a cross-shaped vibrator and sixteen ceramic plates are attached to the top and bottom sides of the brass plate. To find the optimum size for the prototype motor, the stator motions were simulated using ATILA by changing the length and thickness of the ceramics. In the results, the stators commonly had three resonance peaks on the admittance curve; the contact tips of the stator moved at trajectories tangential or normal to these resonance peaks. Elliptical displacements of the tips were obtained at off-resonance frequencies. The maximum displacements at the resonance peaks were compared and the maximum displacements of the contact tips were obtained at a length, width, and thickness of 18, 3, and 1.8 mm respectively. With the fabricated prototype motor, high rotational speeds were obtained by applying relatively low voltages. Speed and torque were increased linearly by increasing the voltage. However, torque decreased when the input voltage went over 24 V.

Keywords Thin ultrasonic motor · Piezo actuator · Cross shaped stator · Four contact tips · Elliptical motion

T. Park · S. Jeong (✉) · H. Chong
Changwon University,
Changwon, Gyeongnam, KOREA
e-mail: ssjeong@changwon.ac.kr

K. Uchino
ICAT, MRI, Pennsylvania State University,
University Park PA16802, USA

1 Introduction

The minimum size of an electromagnetic motor is generally limited to about 1 cm because of the low torque and high rotational speed. To enhance torque and reduce speed, a gearbox must be used. However, this reduces the efficiency of the motor significantly. Furthermore, as the size of electromagnetic motor is reduced, the winding wire thickness must also be reduced, which leads to a significant increase in electrical resistance and Joule heating [1]. Ultrasonic motors can be an alternative to electromagnetic motors for small spaces. Ultrasonic motors can produce high torque at low speed with high efficiency, and they can be applied as a gearless simple motor for small electronic devices such as camera zoom lens or cell phones. In addition, ultrasonic motors produce no electromagnetic interference [2–7].

Recently, demand for small motors has rapidly increased in the area of electronic appliances; research is very active in developing ultrasonic motors, especially for compact camera zoom lens. For the last two decades, traveling wave motors (Shinsei) have been used for camera zoom lens. However, the structure of Shinsei motors is relatively complicated to apply to recent small devices. Therefore, several new zoom mechanisms have been developed and reported [8, 9]. These mechanisms are assembled from a small rotary motor and a screw to linearly move the lens, which is guided by guide rails.

In our previous paper, a new type of ultrasonic rotary motor with a cross-shaped stator was proposed [10]. The elliptical displacements of the four tips, which are produced by bending ceramics, rotate the rotor using friction between the tips and the outer surface of the rotor. If we make a big hole on the rotor as a path for light and attach a zoom lens, this zoom lens can be controlled by the motor.

Using a similar structure, another new type of motor which can be made easily and cheaply is described in this paper. A

thin brass plate is used as a cross-shaped vibrator and sixteen ceramic plates are attached to the top and bottom sides of the brass plate. From this thin stator, elliptical displacements of the four contact tips were obtained. For the design, motions of the stators were simulated using ATILA (ver.5.2.4) and the optimum size was found by changing the length and thickness of the stator ceramics.

2 Structure and principle of the thin cross shape motor

Figure 1 shows the structure of the cross-shaped stator. The stator looks like a cross; two hollow bars are vertically crossed. This motor is named the thin cross-type by virtue of the shape of the stator. As shown in Fig. 2, eight of the sixteen ceramics are attached to the upper face and the other eight are attached to the bottom face of the brass plate. The thickness of the brass plate is 0.2 mm.

By combining the polarization directions of ceramics and the applied electric fields as shown in Fig. 2, the brass plate resonated at various frequencies and elliptical displacements of the four contact tips were obtained.

When ceramics were attached to only one side of the plate, useless three-dimensional fluctuations occurred at the four tips because the brass plate was thin. By attaching ceramics to both sides of the brass plate, stable two-dimensional motions were obtained. At each arms of the brass plate, the top and bottom ceramics produce vibrations symmetrical to the brass surface. Because the ceramics on both sides of the brass plate make the same vibrations, it is enough to explain the principles of the stator by considering only one side. Figure 3(a) shows the directions of polarization and the electric field for the ceramics. Points A, B, C, and D are the contact points between the stator and rotor. As shown in Fig. 3(b), each contact point has two arms with polarized ceramics. By applying two electric fields with a 90° phase difference to the ceramics, each contact point produces rotational displacements, as shown in Fig. 3(c). These rotational displacements are transferred to the rotor by friction between the contact points and surface of the rotor and the rotor can be rotated towards a certain direction.

3 FEA simulations for design stator indicate maximum displacement

The finite element analysis program ATILA (ver.5.2.4) was used to simulate the characteristics of the stator. For vibrating materials, a brass metal plate of 0.2 mm thickness was used with changing lengths and thicknesses for the arms where the ceramics were attached. The metal plate played the role of a common electrode for the ceramics. To allow the four contact tips (points A–D in Fig. 3(a)) freedom to move, the stator was fixed by clamping the middle surfaces where the two arms meet together. Resonance frequencies were found from the admittance curve, and displacements of the four contact tips were calculated for each frequency. Through FEM modal analysis, at resonance frequencies it was found that the tips of the stator draw one of two linear trajectories—normal or tangential—to the surface of a rotor. The actual motor uses elliptical displacement, which can be obtained at off-resonance frequencies. To optimize the size of the stator, the elliptical displacement of the tips must be compared; however, it is incorrect to choose certain frequencies near the resonance. Therefore, the displacements at the resonance frequencies were compared to optimize the size of the stator, using the fact that a bigger linear displacement at a resonance frequency can also produce a bigger elliptical displacement at an off-resonance frequency.

3.1 Displacements depending on the length of the ceramics

The lengths of the ceramics used were 3, 4.5, 6, 7.5, 9, 10.5, 12, 13.5, 15, 16.5, 18, 19.5, 21, 22.5, 24, 25.5, 27, 28.5, and 30 mm, while both the width and thickness were fixed to 3 and 1.5 mm, respectively. For all variations, the thickness of the brass plate was 0.2 mm. These nineteen stators commonly had three resonance frequency peaks between 20 and 200 kHz. At each resonance frequency, the contact tips moved on trajectories tangential or normal to the rotor surface. Because the elliptical motions of the tips were obtained at off-resonance frequencies, it was difficult setting up adequate comparison points. For this reason, the resonance frequency with the maximum displacement was

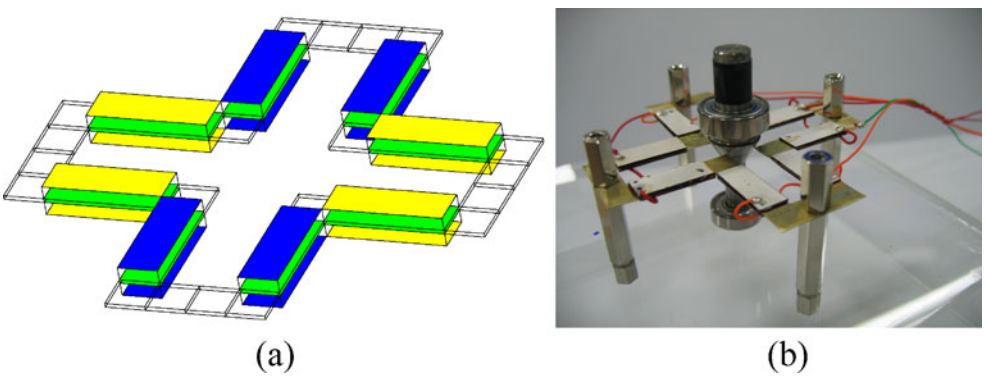

Fig. 1 (**a**) Sixteen ceramics are attached to the top and bottom surfaces of the thin cross-shaped brass plate. The color of the ceramics indicates phases of applied electric fields. (**b**) Photo of a cross-type motor

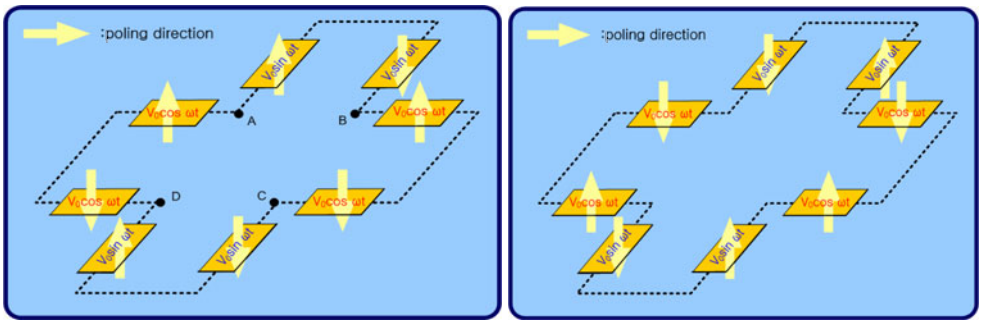

Fig. 2 Polarization and electric fields on ceramics. Arrows indicate the polarization directions, and applied electric fields are shown as sin or cos. (**a**) Ceramics on upper surface. (**b**) Ceramics on bottom surface

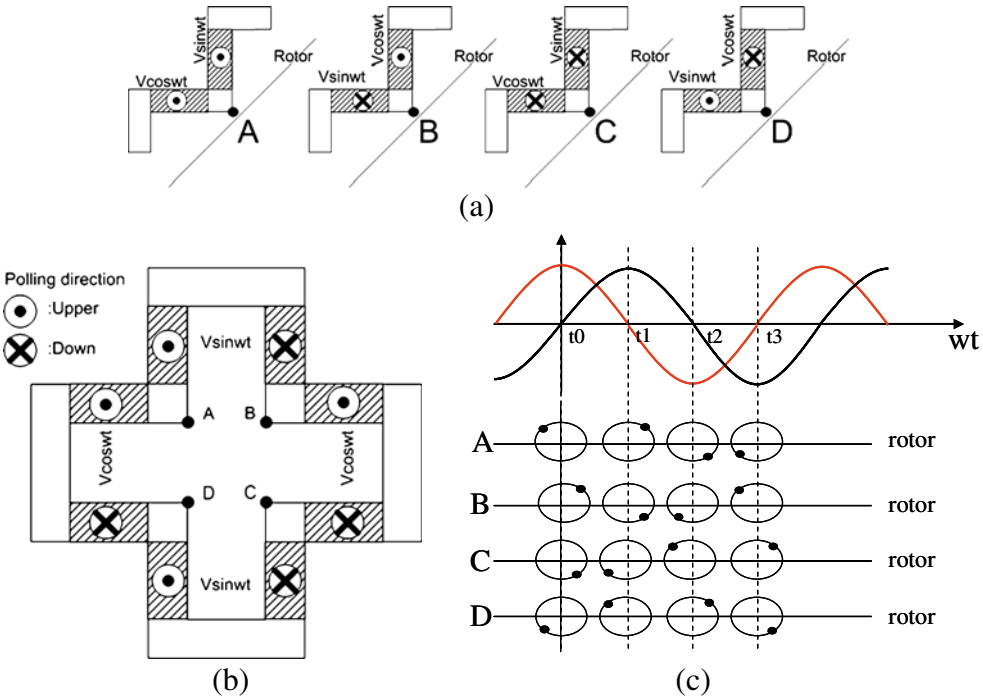

Fig. 3 Generation of elliptical displacements at four contact tips. (**a**) Four contact points on the stator. (**b**) Polarization and electric fields for the ceramics at each contact point. (**c**) Elliptical motions of the contact tips

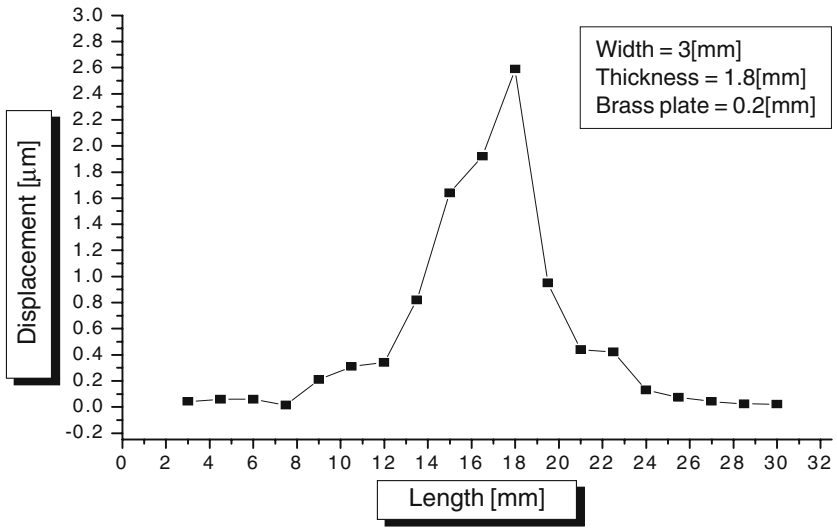

Fig. 4 Change in maximum displacements of the contact tips depending on the length of the ceramics

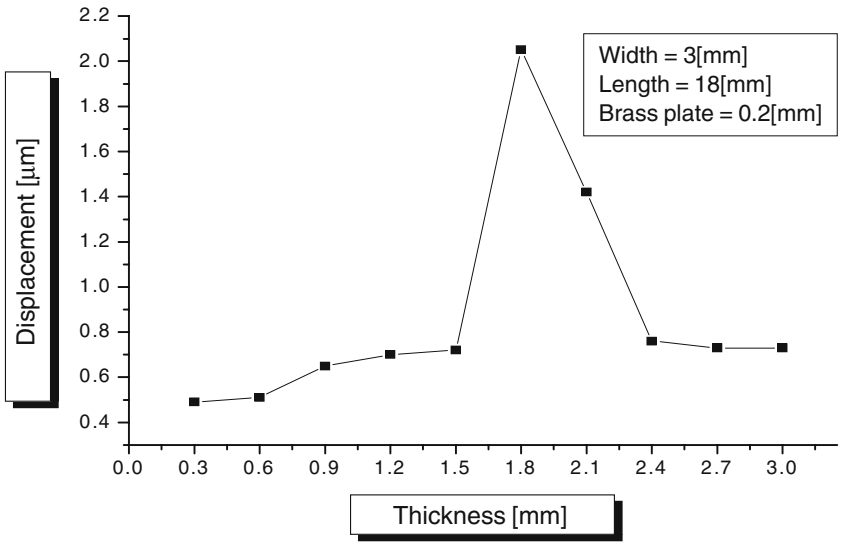

Fig. 5 Change in maximum displacements of the contact tips depending on the thickness of the ceramics

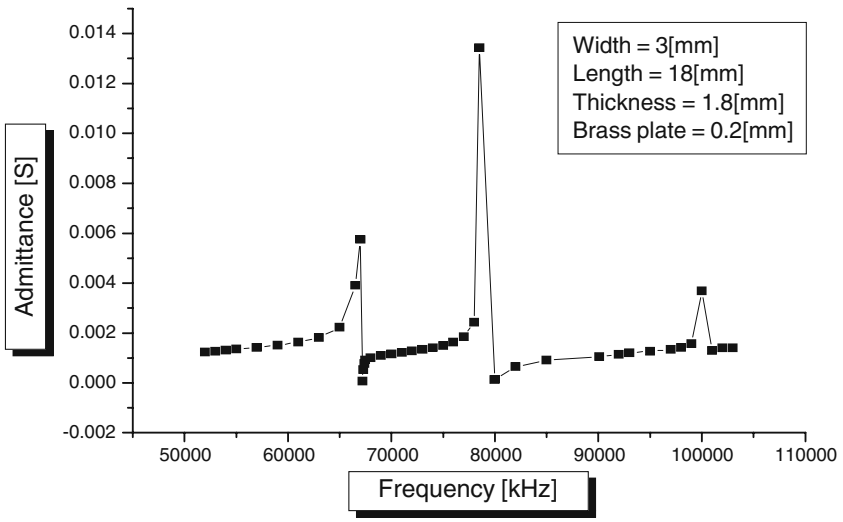

Fig. 6 Change in admittance of the stator depending on the frequency

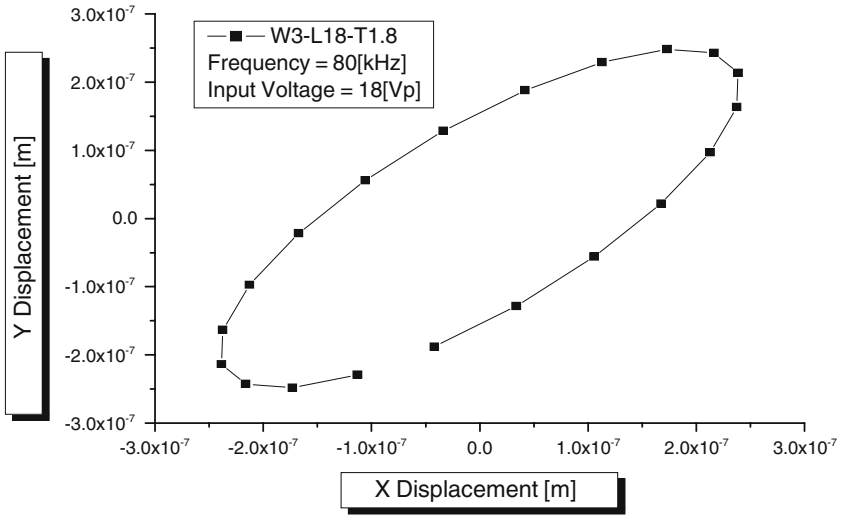

Fig. 7 Elliptical displacement characteristics of the maximum displacement model

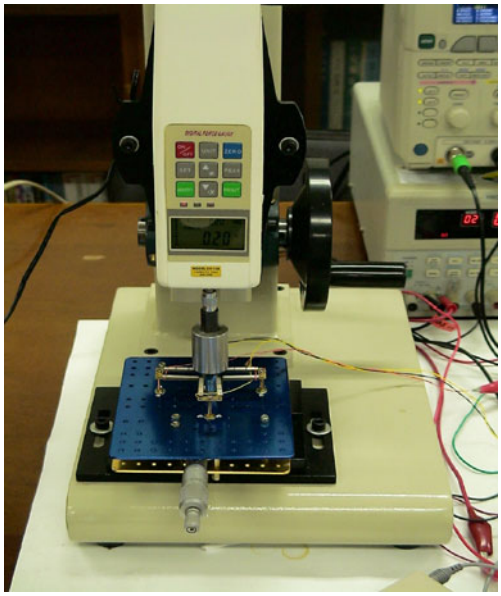

Fig. 8 Measurement equipment using an X-Y stage and push-pull gauge

chosen as a comparison point. Figure 4 shows the changes in maximum displacements of the contact tips depending on the lengths of the ceramics. The maximum displacements of the tips increased with the length until 18 mm, but displacements decreased after this point. These results are consistent with the results for the first cross-type motors [8].

3.2 Displacements depending on the thickness of the ceramics

The thicknesses of the ceramics were changed to 0.3, 0.6, 0.9, 1.2, 1.5, 1.8, 2.1, 2.4, 2.7, and 3 mm, while both the length and width were fixed to 18 and 3 mm, respectively. For all variations, the thickness of the brass plate was 0.2 mm. The results are shown in Fig. 5, and maximum displacement was obtained when the thickness of the ceramics was 1.8 mm.

Figure 6 shows the change in admittance for the selected stator whose size was determined by simulation. There were three peaks of admittance. Through modal analysis, the contact tips of the stator were found to draw linear trajectories either normal or tangential to the surface of a rotor. At the first peak of 67 kHz, the tips move on a normal trajectory; at 78.75 kHz they also move on a normal trajectory; and at 100 kHz, they move on a tangential trajectory. The elliptical motions of the tips were obtained at off-resonance frequencies between these three admittance peaks. Because the maximum displacement was obtained at 78.75 kHz, an off-resonance frequency of 80 kHz was selected from the nearby frequencies of the peak. Figure 7 shows the elleptical displacement of a tip of the stator at 80 kHz. In the *x*-*y* axis charting the elliptical course, torque increases by increasing *x*, and speed increases by increasing *y*.

4 Experiments

A prototype motor was fabricated using the simulation results. The motor was made by attaching ceramics with lengths, widths, and thicknesses of 18, 3, and 1.8 mm respectively on a 0.2-mm thick brass plate. A photo of the fabricated motor is shown in Fig. 1(b). Figure 8 shows the measurement equipment using an X-Y stage and push-pull gauge. Balanced contact between the four contact tips of the stator and the rotor surface was maintained by using the X-Y stage. The rotating shaft of the rotor was combined with a push-pull gauge using a ball bearing. The preload

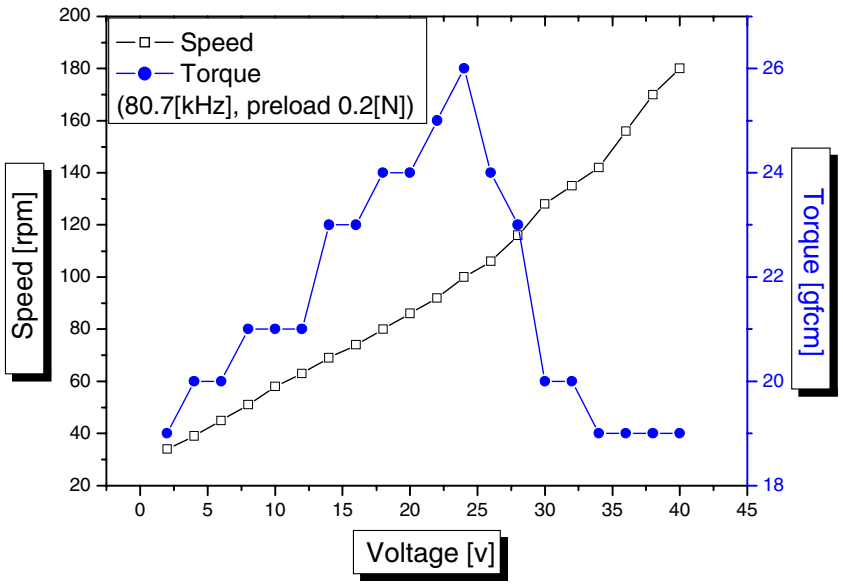

Fig. 9 Rotational speeds and torque of the prototype motor

between the stator and rotor was also controlled and measured with the push-pull gauge. Although the maximum elliptical displacement was obtained at an off-resonance frequency of 80 kHz according to simulations, as shown in Fig. 7, in practice the motor was most powerful at the frequency 80.7 kHz. This difference in frequency may have ben caused during the fabrication process. As shown in Fig. 9, high rotational speed was obtained from the motor by applying relatively low voltages. Speed increased linearly as the voltage increased. Torque also increased until 24 V but decreased after this point.

5 Conclusion

To find the maximum displacement of the newly proposed thin cross-shaped stator, the stator motions were simulated using ATILA and optimized by changing the length and thickness of the ceramics. A prototype motor of the optimum size was then fabricated.

In the results, longer arms for the stator created bigger displacements for the contact tips; however, if the length to width ratio went over 6 (18 mm/3 mm), the displacement of the tips decreased. An adequate thickness for the ceramics was necessary for proper displacements; 1.8-mm thick ceramics attached to a 0.2-mm thick brass plate generated the biggest displacement. Elliptical motions for the contact tips could be obtained at off-resonance frequencies. At resonance frequencies, the contact tips of the stator moved at tangential or normal trajectories. Speed increased linearly with increasing voltage. However, torque decreased when the input voltage went over 24 V. High rotational speed was obtained from the fabricated prototype motor by applying relatively low voltages at the same frequency as simulations.

Acknowledgement This work was supported by the Korea Research Foundation Grant and funded by the Korean government (KRF-2007-313-D00287).

References

1. K. Uchino, *Micromechatronics*. (Marcell Dekker, 2002), p. 5
2. S. Ueha, Y. Tomikawa, M. Kuroaswa, N. Nakamura, *Ultrasonic Motors Theory and Applications*. (Oxford, 1993), pp. 4–7
3. T. Sashida, Trial construction and operation of an ultrasonic vibration driven motor. JJAP **51**, 713 (1982)
4. Y. Tomikawa, T. Ogasawara, Ultrasonicmotors-constructions/ characteristics /applications. Ferroelectrics **91**, 163–178 (1989)
5. K. Uchino, Piezoelectric ultrasonic motors: overview, Smart Mater. Struct 273–285 (1998)
6. H.P. Ko, S.S. Kim, S.N. Borodinas, P.E. Vasiljev, C.Y. Kang, S. J. Yoon, A novel tiny ultrasonic linear motor using the radial mode of a bimorph. Sensors and Actuators A: Physical **125**, 477–481 (2006)
7. H.P. Ko, S.S. Kim, C.Y. Kang, H.J. Kim, S.J. Yoon, Optimization of a piezoelectric linear motor in terms of the contact parameters. Mater. Chem. Phys. **90**, 322–326 (2005)
8. R. Lee, Lobster-auto focusing and zoom. *Proceeding of 47th ICAT/JTTAS Joint International Smart Actuator Symposium*, (2006)
9. D. Handerson, Piezoelectric linear motor for mobile phone cameras. *Proceeding of 47th ICAT/JTTAS Joint International Smart Actuator Symposium*, (2006)
10. H.H. Chong, T.G. Park, M.H. Kim, A study on driving characteristics of the cross type ultrasonic rotary motor. J. Electroceram. **17**, 561–564 (2006)